Paleoceanography and Paleoclimatology

RESEARCH ARTICLE
10.1029/2025PA005211

Special Collection:
Holocene climate changes: process, mechanism and impacts

†Deceased

Key Points:

- Guatemalan speleothem record indicates an extended dry period between 1400 and 1600 CE with abrupt onset and ending
- The beginning of the Mesoamerican dry period coincides with the onset of the Little Ice Age, suggesting a large-scale origin
- Drying occurred when Intra-Americas Sea surface temperatures cooled below the threshold conditions to sustain atmospheric deep convection

Supporting Information:

Supporting Information may be found in the online version of this article.

Correspondence to:

A. Winter,
Amos.Winter@indstate.edu

Citation:

Winter, A., Warken, S., Zanchettin, D., Lachniet, M., Rubino, A., Miller, T., & Cheng, H. (2025). Evidence for persistent drought over Mesoamerica between 1400 and 1600 CE. *Paleoceanography and Paleoclimatology*, *40*, e2025PA005211. https://doi.org/10.1029/2025PA005211

Received 8 MAY 2025
Accepted 14 AUG 2025

Author Contributions:

Conceptualization: Amos Winter, Sophie Warken, Davide Zanchettin
Data curation: Sophie Warken
Formal analysis: Davide Zanchettin
Funding acquisition: Amos Winter, Matthew Lachniet
Investigation: Amos Winter, Sophie Warken, Matthew Lachniet
Methodology: Amos Winter, Sophie Warken, Davide Zanchettin, Matthew Lachniet
Project administration: Amos Winter, Sophie Warken, Davide Zanchettin

Evidence for Persistent Drought Over Mesoamerica Between 1400 and 1600 CE

Amos Winter[1,2,3], Sophie Warken[4,5], Davide Zanchettin[2], Matthew Lachniet[2,6], Angelo Rubino[2], Thomas Miller[7†], and Hai Cheng[8]

[1]Department of Earth and Environmental Systems, Indiana State University, Terre Haute, IN, USA, [2]Department of Environmental Sciences, Informatics and Statistics, University Ca' Foscari of Venice, Mestre, Italy, [3]Department of Marine Sciences, University of Puerto Rico, Mayaguez, PR, USA, [4]Institute of Earth Sciences, University of Heidelberg, Heidelberg, Germany, [5]Institute of Environmental Physics, University of Heidelberg, Heidelberg, Germany, [6]Department of Geoscience, University of Nevada Las Vegas, Las Vegas, NV, USA, [7]Department of Geology, University of Puerto Rico, Mayaguez, Puerto Rico, [8]Institute of Global Environmental Change, Xi'an Jiaotong University, Xi'an, China

Abstract The Little Ice Age (LIA) (c. 1350 to 1850 CE) was a major period of anomalously cold conditions over much of the Earth. However, strong heterogeneity of reconstructed climatic anomalies renders the spatial and temporal characterization of the LIA in the tropics an enduring gap to be filled. Here, we describe hydroclimatic variations reconstructed using a speleothem (GU-Xi-1) from the southern Yucatán peninsula that precipitated aragonite since 1000 CE. Stable oxygen isotope ratios from GU-Xi-1 are interpreted as a proxy for past rainfall amounts, for which they allow to resolve variability on interannual time scales. The reconstructed precipitation record demonstrates drier than normal conditions between around 1400 and 1600 CE, which we term the Mesoamerican Dry Event (MDE) with an abrupt - within two decades - onset and termination. The beginning of the MDE occurred at the same time as estimates of the start of the LIA, indicating that there may be a link between the two events. The MDE is associated with surface cooling of the Intra-Americas Sea: between 1400 and 1600 CE, Caribbean sea-surface temperatures fell below the threshold required to sustain deep atmospheric convection, leading to prolonged drying in Mesoamerica.

Plain Language Summary A 32 cm stalagmite GU-Xi-1 from the Cave of Xibalbá, in the Yucatán Peninsula, was examined to reconstruct local climate variations during the past millennium. The age model using 16 precise U/Th dates from this stalagmite was constructed from three different adjacent sections that grew continuously from 1000 CE to 2000 CE. There is good evidence that the middle section grew during anomalously dry conditions from 1400 CE to 1600 CE, which we term the Mesoamerican Drought Event (MDE). Similar dry conditions were also found in other speleothems and lake records that grew nearby. The beginning of the dry event occurred at the same time as recent estimates of the start of the LIA, suggesting a link. The MDE is associated with surface cooling in the Caribbean Sea, and we suggest a connecting mechanism explaining the sudden onset of the MDE. The progressive ocean cooling brings, around 1400 CE, Caribbean sea-surface temperatures below the threshold to sustain atmospheric convective activity, which is the major source of precipitation in the region. Due to this sudden reduction in convective activity, Mesoamerica faces a prolonged dryness, which lasts until the ocean surface warms again enough to reinitiate substantial convective activity.

1. Introduction

The Little Ice Age (LIA), a multi-centennial period of predominant anomalously cold conditions on Earth, is considered to have profoundly contributed to characterize Earth's climate during the pre-industrial part of the last millennium (e.g., PAGES Hydro2k Consortium, 2017; Fernández-Donado et al., 2013; Mann et al., 2009). Estimates indicate that the LIA occurred from c. 1350 to c. 1850 CE (Guo et al., 2024; Lozano-García et al., 2007; Mann et al., 1999; Matthews & Briffa, 2005). It was originally detected in Northern Hemisphere paleoclimate proxies, but later evidences from the Southern Hemisphere suggest it was a near-global phenomenon (e.g., Simms et al., 2021). While the exact causes of the persistent cooling are not unambiguously known, several factors are thought to have contributed, including external forcing such as reduced solar activity and explosive volcanism (e.g., Lapointe & Bradley, 2021; Moffa-Sánchez et al., 2014; Slawinska & Robock, 2018), and internal feedback

Resources: Amos Winter, Sophie Warken, Davide Zanchettin, Matthew Lachniet, Angelo Rubino, Thomas Miller, Hai Cheng
Supervision: Amos Winter, Sophie Warken
Validation: Sophie Warken, Davide Zanchettin
Visualization: Sophie Warken, Davide Zanchettin
Writing – original draft: Amos Winter, Sophie Warken, Davide Zanchettin, Matthew Lachniet
Writing – review & editing: Amos Winter, Sophie Warken, Davide Zanchettin, Matthew Lachniet, Angelo Rubino, Hai Cheng

mechanisms involving changes in the extent of North Atlantic sea ice, strength of oceanic surface currents as well as atmospheric circulation (e.g., Lapointe & Bradley, 2021; Thirumalai et al., 2018; Zhuravleva et al., 2023).

In Mesoamerica, a number of studies provide evidence for climatic and environmental variations during the last millennium, including the LIA (e.g., Asmerom et al., 2020; Burn & Palmer, 2014; Cuna et al., 2014; Lozano-García et al., 2007; Medina-Elizalde et al., 2010). However, recent compilations also highlighted the heterogeneity in the regional reconstructions - especially during the LIA - which may be predominantly the result of unappreciated climate controls on the climate proxies as well as uncertainties of the chronologies (e.g., Akers et al., 2019; Obrist-Farner et al., 2023; Oster et al., 2019; Steinman et al., 2022; Wogau et al., 2022). Therefore, additional robust proxy reconstructions are needed for the region.

Today, regional precipitation in Mesoamerica is largely confined during the season spanning between June and October, linked primarily to the meridional displacements of the Intertropical Convergence Zone (ITCZ), which reaches latitudes around 15°N in the boreal summer (e.g., Lechleitner et al., 2017; Martinez et al., 2019; Winter et al., 2015). Year-to-year variability is influenced by the interaction of global and regional oceanic and atmospheric processes which determine moisture convergence associated with the ITCZ and the North Atlantic Subtropical High (Martinez et al., 2019). The Caribbean low-level jet (Taylor et al., 2013) and the Atlantic Warm pool (Wang et al., 2006) further modulate regional precipitation patterns in time and space (Martinez et al., 2019; Wang et al., 2013).

Among climate archives, speleothems can be precisely dated and ideally have few sources of proxy uncertainty. $\delta^{18}O$ records have been shown to provide reliable records of convective activity and regional rainfall amount in Mesoamerica and the Caribbean area (e.g., Medina-Elizalde et al., 2010; Vieten, Warken, Winter, et al., 2024; Winter et al., 2020), hence allowing to constrain hydroclimate evolution during the LIA on the Yucatán peninsula (Hodell, Brenner, Curtis, et al., 2005; Steinman et al., 2022; Winter et al., 2015).

Herein, we present an extended speleothem $\delta^{18}O$ time series from a precisely-dated aragonite stalagmite from Xibalbá cave, Guatemala (Figure 1) showing a pronounced layer of deposited carbonate and a positive $\delta^{18}O$ excursion that describes a 200-year persistent dry period. We present the proxy data and the age model used for the reconstruction (Section 2), illustrate the rapid transition revealed by the data to persistent, exceptionally dry conditions around 1400 CE that quickly terminated around 1600 CE - the Mesoamerican Dry Event (MDE) - and place our record within the context of other regional paleoclimate records that span the LIA (Section 3) to characterize the MDE, and discuss possible mechanisms responsible for the event (Section 4).

2. Materials and Methods

2.1. The GU-Xi-1 Speleothem

The 32 cm-long speleothem GU-Xi-1 (Figure 1) was recovered in 2007 from Xibalbá cave (approx. 17.5°7′48″N, 88°51′57″W, Figure 2) located in the Campur Formation at an elevation of 350 m asl in the Maya Mountains bordering both Guatemala and Belize. GU-Xi-1 was collected ~250 m inside the cavern and was active and dripping at the time of collection. The speleothem was chosen for its candle-shape, its distance from outside atmospheric influences, and its location of 30 m above the nearby modern river level; the karst surface is generally 100–150 m above the cave passages (Winter et al., 2015). GU-Xi-1 consists of three clearly visible sections (Figure 1) labeled A (upper), B (middle) and C (lower). Noteworthy is the 11° offset of the growth axis from section C to A. We postulate that this may have been caused by a change in the drip orientation after the large earthquake of 1541 CE (compare age model in Figure 1c).

2.2. U/Th Dates and Age Model

200 mg of powder were collected with a hand-held dental drill from a polished slab section of GU-Xi-1 along growth layers for dating. Three dates were obtained from section B and four from section C (Table 1). The nine dates comprising section A were previously described in Winter et al. (2015). The dates were either obtained from a Finnigan Element ICP-MS (Table 1 Section A; samples GUA 1–6), a Finnigan Neptune MC-ICP-MS (Table 1 Section A, samples GUA 8–13), or a Nu Plasma Element (Table 1 Section B and C) at the University of Minnesota. Activity ratios were calculated using the half-lives from Cheng et al. (2013), and all errors are reported at the 2σ-level. Based on the dates, a chronology with uncertainty (Figure 2) was built with the software COPRA (Breitenbach et al., 2012) using 2,000 Monte Carlo simulations. According to the U/Th dates section C grew from

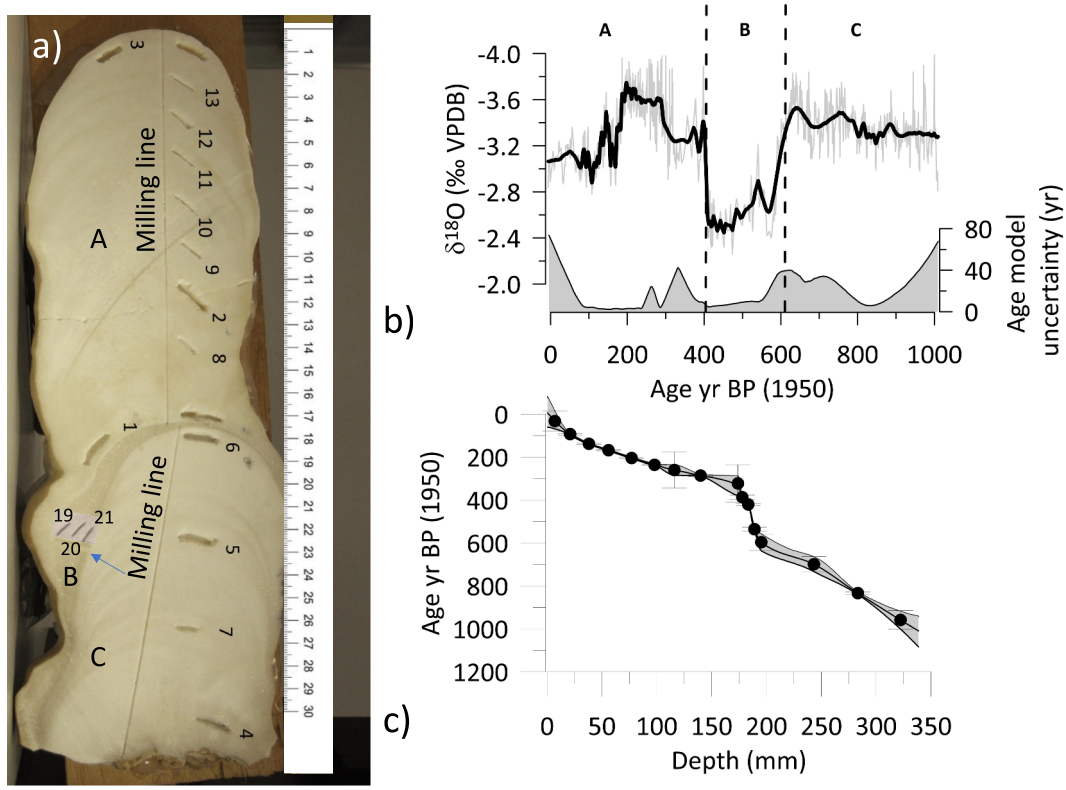

Figure 1. Image of speleothem GU-Xi-1, proxy data, and age model construction; (a) Entire GU-Xi-1 speleothem (ruler in cm) showing all three sections mentioned in our study: (A) upper, (B) middle, (C) lower. The numbers refer to the U/Th dates in Table 1. Clearly visible is the change in growth axis of 11° between sections A and C. (b) δ^{18O} over the entire record with age model uncertainty; (c) age model using COPRA.

c. 1000 to 1400 CE, section B from c. 1400 to 1600 CE and section A from c. 1600 to 2000 CE. Before and after the change in drip axis GU-Xi-1 growth rates were 0.35 mm/yr and 0.58 mm/yr, respectively. Section A, covering the years from c. 1700 to 2000 CE, was already reported extensively in Winter et al. (2015).

2.3. Isotopic Analysis

Stable oxygen isotopes samples for all sections of GU-Xi-1 were extracted and analyzed in the same way as described in Breitenbach and Bernasconi (2011). Briefly, sections A and C were continuously milled (Figure 1a) along the central growth axis at 0.3 mm intervals. 482 samples were collected corresponding to an approximate yearly to bi-yearly resolution. Samples were analyzed using a continuous flow isotope ratio mass spectrometry at ETH Zurich, Switzerland. The external analytical precision for $\delta^{18}O$ is smaller than 0.06‰. For section B, 65 samples each containing about 200 µg of powder were continuously milled at 0.1 mm intervals along the angled growth axis of 2 cm, resulting in a 4-year resolution for the stable isotope data. An internal standard was used every 5th sample for drift correction. Samples were heated in the Gasbench tray to 72 ± 0.1°C, and analyzed on a Gasbench II carbonate periphery, coupled to a Delta V Plus mass spectrometer (both Thermo Electron Corporation, Bremen, Germany).

2.4. Climatology

The modern climatology of the region was described at length in Winter et al. (2015). One of the most salient features is the rainy season, that occurs in the highlands of Guatemala between June and October (Giannini et al., 2000). Rainfall originates usually from the vicinity of the ITCZ via transport into the monsoonal system via the Caribbean low-level jet, and by localized convection. Year-to-year rainfall variability in the Guatemala mountain regions today is correlated with the gradient between sea-surface temperatures (SSTs) in the western tropical Atlantic and eastern tropical Pacific. Colder (warmer) than normal tropical Atlantic SSTs that are

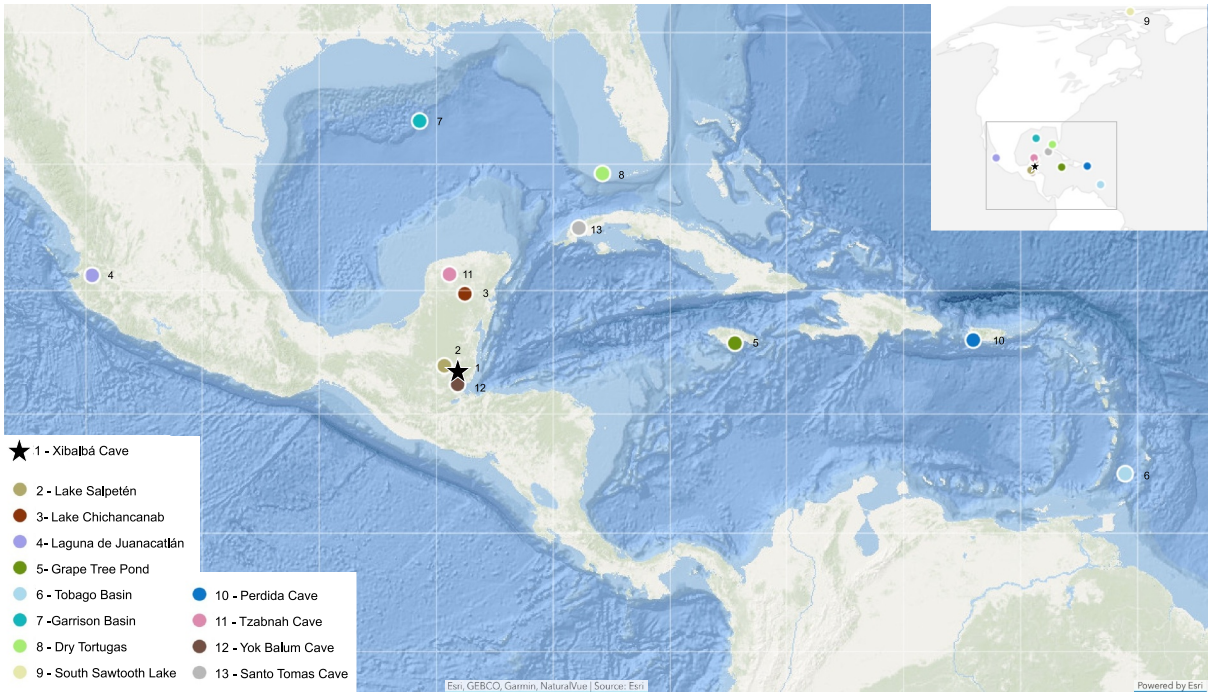

Figure 2. Regional map showing the location of GU-Xi-1 (blue star) from Xibalbá, Guatemala/Belize border (1) compared to the locations of other paleoclimate records used in this study: (2) Lake Salpetén (Rosenmeier, Hodell, Brenner, Curtis, & Guilderson, 2002); (3) Lake Chichancanab, Mexico (Hodell, Brenner, & Curtis, 2005); (4) Laguna de Juanacatlan (Metcalfe et al., 2010); (5) Grape Tree Pond, Jamaica (Burn & Palmer, 2014); (6) Tobago Basin, Caribbean (Zhuravleva et al., 2023); (7) Garrison Bay, Gulf of Mexico (Thirumalai et al., 2018); (8) Dry Tortugas, Gulf of Mexico (Lund & Curry, 2006); (9) South Sawtooth Lake (Lapointe et al., 2020); (10) Perdida Cave (Winter et al., 2011; (11) Tzabnah Cave, Mexico (Medina-Elizalde et al., 2010); (12) Yok Balum Cave, Belize (Asmerom et al., 2020; Kennett et al., 2014); (13) Santo Tomas Cave, Cuba (Fensterer et al., 2012). Colors are coded to represent the same colors used in the graphs of Figures 3 and 4 and Figure S2 in Supporting Information S1.

consistent with a stronger (weaker) and more southward (northward) displaced North Atlantic Subtropical High, lead to drier (wetter) than normal conditions in Central America. Similarly, anomalously warm (cold) eastern equatorial Pacific SSTs, for example, during El Niño (La Niña) events, force an equatorward (northward) displacement of the east Pacific ITCZ and contribute to drying (wetting) in most of Central America (Lachniet et al., 2007; Seager et al., 2009).

3. Results

3.1. GU-Xi-1 Age Model

GU-Xi-1 consists of aragonite generally unaffected by post-depositional diagenetic alteration, with high levels of U concentrations ranging from 1140 to 3226 ppb (Table 1). As there is also very little detrital ^{230}Th, the ages have small error bars in the range of a few years for the MC-ICP-MS ages, and around 30–40 years for ICP-MS measurements. The sections have an age control point approximately every 30–40 years. Supporting the U/Th dating is the fact that the speleothem exhibits visible annual layers (Figure 1a) that match closely the U/Th dating within a few years (Figure S1 in Supporting Information S1). The age model obtained with COPRA (Figure 1c) indicates that the average growth rate of section A was 0.58 mm/yr, section B 0.35 mm/yr, and section C 0.35 mm/yr. The middle section B growth rate is dependent on the location where the samples were taken. Since this was one of the larger cross sections, we consider this an upper limit.

3.2. Stable Isotopes

δ^{18}O values of GU-Xi-1 range from −3.7 ‰ to −2.4 ‰ VPDB (Figure 3a). The most notable feature is a long positive excursion associated with section B that exhibits more positive δ^{18}O values that are about 0.8 ‰ heavier than the values to either side. The period of heavy oxygen isotope values starts rather rapidly c. 1385–1441 CE (5–95 percentile interval for the date of the first sample exceeding −2.8 ‰) and ends c. 1590–1600 CE (5–95

Paleoceanography and Paleoclimatology

10.1029/2025PA005211

Table 1
^{230}Th Dating Results

Section	Sample ID	Weight g	Depth mm	^{238}U ppt		^{232}Th ppt		[^{230}Th/^{232}Th] ppm		δ^{234}U measured		[^{230}Th/^{238}U] activity		Age uncorrected		Age corrected		$\delta^{234}U_{initial}$ corrected		Years AD
A	*GUA3*	0.1054	7.0000	2,407	±7	105	±6	173.4	±241.0	481.6	±3.6	0.00046	±0.00063	33.7	±46.8	32.8	±46.8	481.7	±3.6	1,976.2
A	*GUA13*	0.0701	21.0000	3,202	±5	819	±17	86.7	±2.9	489.7	±1.9	0.00134	±0.00004	98.5	±2.6	93.5	±4.4	489.8	±2	1,915.54
A	*GUA12*	0.0787	38.0000	2,998	±4.3	225	±5	414.9	±11.7	492.8	±1.8	0.00188	±0 00004	137.8	±2.6	138	±2.8	493	±1.8	1,871
A	*GUA11*	0.0641	56.0000	3,226	±6	209	±5	589.7	±16.3	492.4	±2.2	0.00232	±0.00004	169.7	±2.9	168.5	±3	492.6	±2.2	1,840.54
A	*GUA10*	0.067	77.0000	3,341	±5.1	216	±5	711.4	±19.0	499.5	±1.8	0.00279	±0.00004	203.1	±3.2	204	±3.3	499.8	±1.8	1,805
A	*GUA9*	0.0765	98.0000	2,891	±4	334	±7	463.2	±11.0	487.8	±1.8	0.00325	±0.00004	238.1	±2.8	235.9	±3.2	488.2	±1.8	1,773.14
A	*GUA2*	0.1,083	116.0000	1,290	±3	11	±6	6,629.5	±4,185.3	491.5	±3.6	0.00355	±0.00115	259.9	±84.5	259.7	±84.5	491.9	±3.6	1,749.3
A	*GUA8*	0.0698	140.0000	2,941	±5.6	545	±11	350.8	±8.2	491.3	±2.2	0.00394	±0.00005	288.7	±3.4	286	±4.3	491.7	±2.2	1,723
A	*GUA1*	0.1199	174.0000	1,140	±2	28	±6	3,011.9	±1,012.9	490.6	±2.4	0.00441	±0.00118	323.2	±86.9	322.7	±86.9	491.1	±2.4	1,686.3
B	*GUA19*	*0.0437*		*3,129*	*±8.3*	*1,809*	*±36*	*153.4*	*±3.9*	*474.3*	*±3.1*	*0.0054*	*±0.0001*	*398*	*±6*	*387*	*±10*	*475*	*±3*	*1,625*
B	*GUA 20*	*0.0463*		*3,071*	*±4*	*1,038*	*±6*	*1,038*	*±26*	*482.1*	*±2.1*	*0.0057*	*±0.0001*	*421*	*±5*	*420*	*±5*	*483*	*±2*	*1,592*
B	*GUA 21*	*0.0429*		*2,584*	*±5.4*	*213*	*±30*	*213*	*±5*	*488.1*	*±2.4*	*0.0074*	*±0.0001*	*547*	*±7*	*536*	*±10*	*489*	*±2*	*1,476*
C	*GUA6*	0.0997	185.0000	3,146	±6	75	±7	5,634.2	±621.5	488.4	±2.4	0.00812	±0.00052	597.2	±38.6	596.7	±38.6	489.2	±2.4	1,412.3
C	*GUA5*	0.1174	225.0000	3,030	±8	75	±6	6,341.4	±574.8	484	±3.1	0.00949	±0.00047	699.9	±34.7	699.4	±34.7	485	±3.1	1,309.6
C	*GUA7*	0.0704	264.4000	2,892	±4.2	760	±15	732.4	±15.2	504.7	±2.1	0.01154	±0 00006	839	±4.0	834	±6	505.8	±2.1	1,175
C	*GUA4*	0 0974	313.4000	3,133	±8	1,221	±8	571.9	±25.6	532.3	±3.2	0.0135	±0.00060	965.8	±43.1	958.4	±43.4	533.8	±3.2	1,050.6

Note. Speleothem GU-Xi-1 U/Th dates for section A, B, C. The dates were obtained from Finnigan Element ICP-MS with errors of 40–80 years and a Finnigan Neptune MC-ICP-MS with errors ≤4 years. U decay constants: $\lambda_{238} = 1.55125 \times 10^{-10}$ (Jaffey et al., 1971) and $\lambda_{234} = 2.82206 \times 10^{-6}$ (Cheng et al., 2013). Th decay constant: $\lambda_{230} = 9.1705 \times 10^{-6}$ (Cheng et al., 2013). $\delta^{234}U = ([^{234}U/^{238}U]$ activity–1) × 1,000. δ^{234}Uinitial was calculated based on ^{230}Th age (T), that is, $\delta^{234}\text{Uinitial} = \delta^{234}\text{Umeasured} \times e^{\lambda 234 \times T}$. Corrected ^{230}Th ages assume the initial ^{230}Th/^{232}Th atomic ratio of $4.4 \pm 2.2 \times 10^{-6}$. Those are the values for a material at secular equilibrium, with the bulk earth ^{232}Th/^{238}U value of 3.8. The errors are arbitrarily assumed to be 50%.

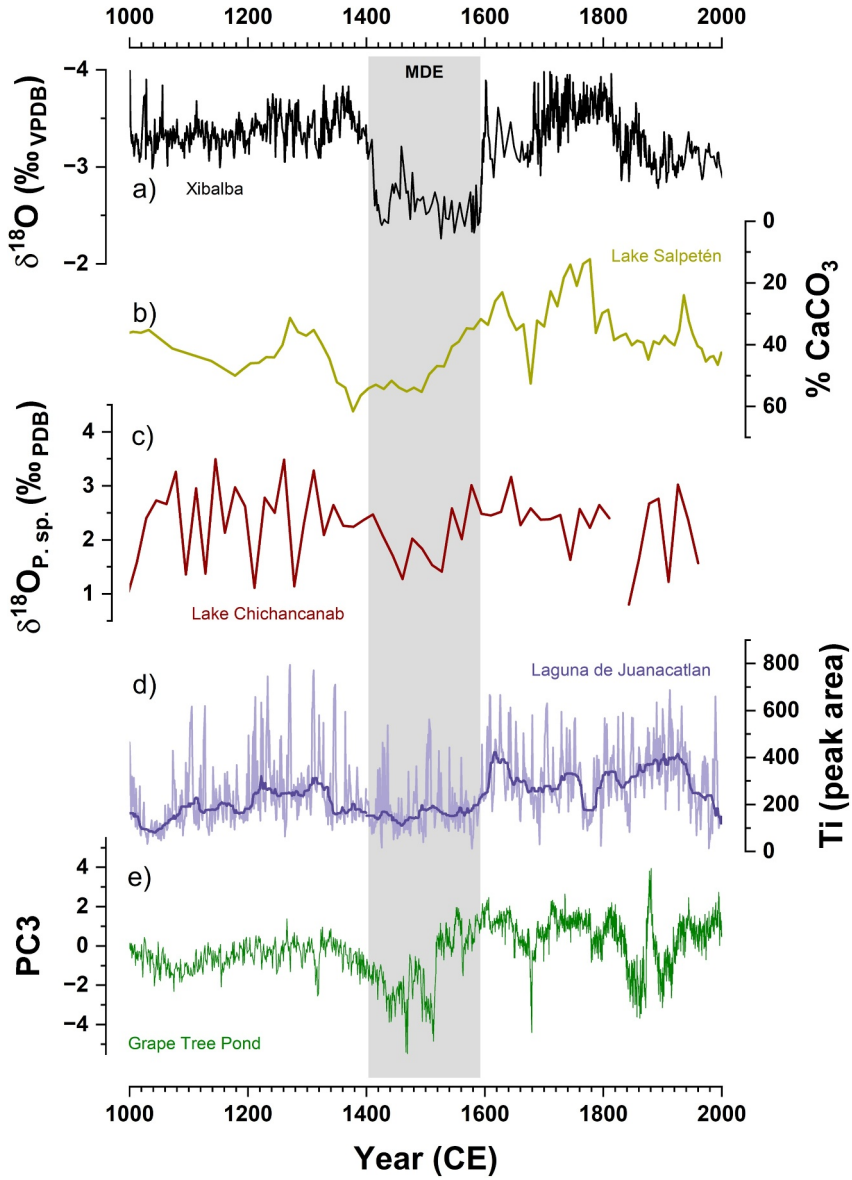

Figure 3. Comparison between the GU-Xi-1 record and relevant regional proxy records. (a) GU-Xi-1 $\delta^{18}O$ record (1); (b) Salpeten $\%CaCO_3$ (2), (Rosenmeier, Hodell, Brenner, Curtis, & Guilderson, 2002); (c) Chichancanab $\delta^{18}O$ (3), (Hodell, Brenner, & Curtis, 2005); (d) Laguna de Juanacatlan Ti values (4), (Metcalfe et al., 2010) and (e) Grape Tree Pond, Jamaica (5), (Burn & Palmer, 2014). The gray band highlights the Mesoamerican Dry Event|Mesoamerican Drought Event. All records are aligned so that up is wet according to the author's original interpretations. Individual numbers before each reference refers to location of record in Figure 2.

percentile interval for the date of the last sample exceeding −2.8 ‰). A strong inverse correlation between speleothem $\delta^{18}O$ and tropical precipitation intensity (Dansgaard, 1964) has previously been observed for the region. This is known as the "amount effect" and is the basis for tropical hydrological reconstruction (Lucia et al., 2024). The significant correlation between the GU-Xi-1 $\delta^{18}O$ time series and observed June-November precipitation in Belize City confirms that the amount effect dominates the GU-Xi-1 signal (Winter et al., 2015). More positive speleothem $\delta^{18}O$ values are commonly interpreted to indicate drier conditions via the amount effect in the tropics (Lachniet & Patterson, 2009), suggesting an extended drought event occurred in that region.

3.3. Comparison With Local Terrestrial Records

Robust high-resolution climate records in Mesoamerica are challenging to find, especially those that grew continuously since the LIA. Also, young tropical speleothems are sometimes hard to date (e.g., Akers et al., 2019; Fensterer et al., 2010; Kerber et al., 2025). Nevertheless, terrestrial hydroclimate reconstructions exist that support the record of GU-Xi-1 (Figure 3). One record using Ti as a precipitation proxy from Laguna de Juanacatlan, Mexico (Metcalfe et al., 2010) exhibits an extended major dry period practically coinciding with that of GU-Xi-1 (Figure 3d). Other lake records, including Salpetén, Guatemala (Rosenmeier, Hodell, Brenner, Curtis, & Guilderson, 2002; Rosenmeier, Hodell, Brenner, Curtis, Martin, et al., 2002, Figure 3b), and Chichacanab from the northern Yucatán peninsula (Hodell, Brenner, & Curtis, 2005, Figure 3c), and Grape Tree Pond from Jamaica (Burn & Palmer, 2014, Figure 3e) as well as La Alberca maar lake, Mexico (Wogau et al., 2019) and Lake Azuei, Haiti (Noncent et al., 2023) display unusually dry intervals for most or part of the MDE. Some speleothem records from the Yucatán peninsula, including two $\delta^{18}O$ data sets from near-by Yok Balum Cave (YOK-I and YOK-G, Asmerom et al., 2020; Kennett et al., 2012) as well as stalagmite "Chaac" from Tzabnah Cave in the northern part of the Yucatán peninsula (Medina-Elizalde et al., 2010) show either unclear or at least slightly drier or cooler periods around 1400–1600 CE (Figure S2 in Supporting Information S1).

3.4. Comparison With Records From the Greater Caribbean Region

Multi proxy-based SST reconstructions from several locations throughout the nearby Intra- Americas Sea indicate that winter SSTs were at least 2°C cooler during the LIA (e.g., Black et al., 2007; Richey et al., 2009; Thirumalai et al., 2018). Several studies using foraminiferal SST proxies including Tobago basin, Caribbean Sea (Zhuravleva et al., 2023, Figure 4d), Garrison basin, northern Gulf of Mexico (Thirumalai et al., 2018, Figure 4e) as well as offshore Puerto Rico (Nyberg et al., 2002, not shown) or at dry Tortugas, Florida Strait (Lund & Curry, 2006, Figure 4f) highlight anomalously cold conditions between 1400 and 1600 CE. Finally, this period is also evident in the annually laminated sedimentary record from Ellesmere Island, Canada, indicating that cool SSTs prevailed in the whole North Atlantic (Lapointe et al., 2020, Figure 4e). Hence, overall cooler SSTs are reported for the Caribbean and the wider North Atlantic basin during the time when GU-Xi-1 $\delta^{18}O$ values indicate drier conditions in Mesoamerica.

4. Discussion

4.1. Proxy Evidence of the Mesoamerican Dry Event

We are confident that the Xibalbá time series is robust and that the combined mineralogy and isotope results support a dry event that occurred between 1400 and 1600 CE. The high uranium content of the stalagmite ensures that the onset and ending dates of the event are well confined, while the dating strongly indicates that deposition occurred nearly continuously throughout this period without apparent growth interruptions (Figure 2 and Section 2.3).

One evidence for drier conditions between 1400 and 1600 CE is that the stable oxygen isotopes in this period are anomalously positive (+0.8 ‰), which is what one would expect from reduced convective activity via the amount effect (e.g., Bernal et al., 2023; Lachniet & Patterson, 2009; Medina-Elizalde et al., 2010; Winter et al., 2020, see Section 2.1). However, we acknowledge that this positive offset in $\delta^{18}O$ values is likely exacerbated by additional effects, such as changes in the kinetics of deposition or disequilibrium fractionation effects (Lachniet, 2015; Vieten, Warken, Zanchettin, et al., 2024; Warken et al., 2020). XRD analyses showed that the speleothem consists of 100% primary aragonite. We also plotted the relationship between $\delta^{18}O$ and $\delta^{13}C$ in all three sections of the Xibalbá speleothem (Figure S3 in Supporting Information S1) and found that all sections displayed similar trends. The trend in section B is in fact nearly identical to that of section A. This supports our finding that there are likely no secondary effects such as recrystallization of aragonite, primary calcite precipitation or other diagenetic effects affecting oxygen isotope fractionation.

We determined both visually and petrographically that the mineralogical structure of section B is equivalent to the speleothem "L layer"-type identified by Railsback et al. (2013). Such fabric is deposited only under exceptionally dry conditions when drip rates slow down to minimum levels. Further evidence is the relatively slow growth of this section which can indicate lower rainfall. This structure only forms when there is not enough time to form a suitable site for carbonate precipitation because of extremely dry conditions. Hence, it is possible that the isotopic

composition of the "L layer" of section B was geochemically altered toward higher values by kinetic and/or disequilibrium effects due to very slow growth, slow drip rates, and evaporation (e.g., Carlson et al., 2020; Deininger et al., 2012; Hansen et al., 2019). We milled the samples for isotope analysis from the widest part of section B. This facilitated acquiring the largest number of samples for analysis. It is difficult to ascertain how far these samples were located from the central growth axis (if there was any). Still, stable isotopes values may become more positive away from the central drip line (Mickler et al., 2006).

In summary, the mineralogical structure of the type of "L Layer" deposition and the more positive stable isotope values in section B indicate generally dry conditions during that time. However, we acknowledge that the values measured in the speleothem may be the result of superimposing effects of less (convective) precipitation (i.e., the "amount effect") and additional kinetic and/or disequilibrium isotopic fractionation, which may have altered the isotope value of the infiltrating meteoric water to even more positive values.

4.2. Regional Reconstruction Differences

Hydroclimate reconstructions suffer from low resolution or inherent limitations. For example, local effects arising from karst-hydrological flow path differences or disequilibrium fractionation processes are one possible explanation of sometimes divergent isotopic time series in stalagmites (e.g., Deininger et al., 2012; Skiba & Fohlmeister, 2023; Treble et al., 2022). In addition, in many cases low U concentrations (and high initial Th) make dating of comparably young material challenging (e.g., Fensterer et al., 2012; Akers et al., 2019; Kerber et al., 2025). Yok Balum cave, located in the same vicinity as Xibalbá provides two well-known records (Figures 2d and 2e) YOK-I (Kennett et al., 2014) and YOK-H (Asmerom et al., 2020). Comparison of these two $\delta^{18}O$ records leaves open the possibility that the signal is also affected by local hydrological processes, land-use changes, or karst effects, potentially limiting its reliability as a direct climate proxy. For speleothems, local cave conditions such as sensitivity to temperature rather than hydrological changes, drip-site specific karst-hydrological differences but also the cave position relative to the primary wind (hence moisture) direction may contribute to explaining inconsistencies across different cave sites, but also to other proxy records from lakes and sediments (e.g., Baker et al., 2019; Bernal et al., 2023; Cuna et al., 2014; Lases-Hernandez et al., 2020; Skiba & Fohlmeister, 2023; Treble et al., 2022; Vieten, Warken, Winter, Schröder-Ritzrau, et al., 2018).

Lake sediment records often contain larger chronological uncertainties because of challenges with radiocarbon dating, due to organic matter cycling, reworking, and calibration of ages, compared to our precise aragonite U-series ages. The presence of opposing hydroclimate anomalies in $\delta^{18}O$ values over short distances is difficult to reconcile without considering non-climatic influences that may compromise the reliability of one or both records. Lake sediment proxies may also be more sensitive to changes in evaporation than rainfall amount and may be further influenced by human land use (Douglas et al., 2012; Rosenmeier, Hodell, Brenner, Curtis, & Guilderson, 2002; Rosenmeier, Hodell, Brenner, Curtis, Martin, et al., 2002). Nevertheless, some of the lake sites, in particular Chichancanab and Juanacatlán, show some similarity with our site (though not with Salpetén). Handling age uncertainty that facilitates comparisons between paleorecords such as lake sediment and speleothem records (e.g., Blaauw & Christen, 2011) is possible but beyond the scope of the present work. A large study of 48 records states that northern hemisphere records are much more heterogeneous that those from the southern hemisphere (Steinman et al., 2022). This seems to be especially the case for the terrestrial Mesoamerican region because of greater complexity of topographic and oceanic influences (Obrist-Farner et al., 2023; Oster et al., 2019; Wogau et al., 2022).

Since Xibalbá matches many reconstructions in the region (detailed below), we believe that it is less affected by such issues. However, for most cave sites including Xibalbá there are not enough data to elucidate some of these local processes, e.g., from comprehensive monitoring studies (e.g., Bernal et al., 2023; Lases-Hernandez et al., 2019; Lases-Hernandez et al., 2020; Vieten, Warken, Winter, Scholz, et al., 2018).

The comparison of available proxy-based hydroclimatic records over Mesoamerica reveals a large similarity to our Xibalbá record (Sections 3.3). Many regional records indicate rather drier than wetter conditions in Mesoamerica between 1400 and 1600 CE, coinciding with relatively cool regional SSTs (Section 3.4). Evidence for environmental degradation in Mesoamerica between c. 1400 and 1600 CE also comes from historical records, reporting frequent droughts concomitant with demographic and epidemiologic disasters, in particular during the 16th century (e.g., Acuña-Soto et al., 2002; Mendoza et al., 2005; Stahle et al., 2011). Some more distant records from the Greater Antilles such as stalagmite $\delta^{18}O$ values from Puerto Rico (Winter et al., 2011), western Cuba

(Fensterer et al., 2012) or Lake Azuei from Haiti (Noncent et al., 2023) also suggest a relatively dry period before c. 1600 CE within age model uncertainties (compare also Figure S2 in Supporting Information S1). Even though the different locations, archives, and proxy types appear to exhibit varying sensitivity to hydroclimatic changes across this period, the regional comparison suggests that the dry interval between c. 1400 and 1600 CE was not confined to the southern Yucatán peninsula but was likely a regional-scale drying event (the MDE) that occurred within a phase of hemispheric cooling and drying (Steinman et al., 2022).

We regard the overall correspondence between Xibalbá and the many records farther afield a good indication that the drying described by the GU-Xi-1 record did occur and was not just a local effect but resulted from a wider regional to hemispheric pattern. Since the agreement appears to be better with records from small islands or SST reconstructions, we surmise this is because these are less affected by the above-mentioned local factors. Hence, we conclude that the Xibalbá dry period is the local expression of a regionally widespread hydroclimate response to cooler SSTs in the tropical Atlantic and Caribbean Sea during the LIA.

4.3. Causes of the Guatemalan MDE

The beginning of the MDE in our record (c. 1385–1441 CE) superposes, within age error, to estimates of the start of the LIA (e.g., PAGES Hydro2k Consortium, 2017; Lozano-García et al., 2007; Matthews & Briffa, 2005) suggesting a link between the two events. But there is still much conjecture regarding attribution and origin of the LIA, as well as hydroclimatic responses on different temporal and regional scales (Cuna et al., 2014; Zhuravleva et al., 2023).

During the LIA, rainfall anomalies in the Western Hemisphere have been associated with concomitant weakening of North Atlantic surface currents and increased Caribbean salinification (e.g., Lapointe & Bradley, 2021; Lund & Curry, 2006; Thirumalai et al., 2018; Zhuravleva et al., 2023). These variations in the large-scale oceanic surface circulation have been linked with changes in the strength of the subpolar gyre and the Labrador Sea Water formation (Marchitto & deMenocal, 2003; Zhuravleva et al., 2023). Reduced convection and surface circulation in the North Atlantic likely triggered the expansion of sea ice in the North Atlantic during the LIA, which combined with reduced meridional salt transfer and sea ice-ocean feedbacks reinforced the initial transient cooling (Lehner et al., 2013; Moffa-Sánchez et al., 2019; Moffa-Sánchez & Hall, 2017; Zhuravleva et al., 2023). This process manifested in persistently cool conditions lasting from 1400 until the early 1600s (Lapointe et al., 2020, Figure 4g).

Several hypotheses have been put forward to explain the dry conditions in Mesoamerica as a result of LIA cooling in the Atlantic basin. Colder SSTs in the (tropical) North Atlantic are linked with a smaller Atlantic Warm Pool, which has been associated with generally weaker precipitation in the region (Wang et al., 2006). Likewise, an intensification/expansion of the North Atlantic Subtropical High caused simultaneous strengthening of the northeast trade winds as well as southward shifts in tropical storm tracks and the ITCZ (e.g., Black et al., 1999; deMenocal et al., 2000; Nyberg et al., 2001; Rauscher et al., 2008; Richey et al., 2009). In addition, the overall synoptic patterns at the time may also have changed when troughs of cold air moved further south than present (Winter et al., 2000). Caribbean cooling further favors an increased pressure gradient between the Atlantic and Pacific basins, leading to a stronger atmospheric moisture transport across Central America (Wang et al., 2013). The interbasin gradient argument was also identified in a proxy-model study by Bhattacharya and Coats (2020). These interacting processes likely contributed to increased dryness in the circum-Caribbean land and Central America between 1400 and 1600 CE.

The GU-Xi-1 record indicates that both the initiation and the termination of the MDE were abrupt, within perhaps 20 years. This behavior points to a threshold response, analogous to what was described by Winter et al. (2020). The cooling in the Intra-Americas Sea may have been up to 2–3°C cooler on average compared to today (Nyberg et al., 2002; Richey et al., 2009; Zhuravleva et al., 2023). Thus, the present-day range of 26–29.5°C decreased to about 24 to about 27.5°C.

A convection threshold response (Winter et al., 2020) could explain the sudden onset of the drying events as SST may have fallen below a level needed to trigger local moist convection (Williams et al., 2009). As a result, convective activity was too small, especially in areas located in the leeward sides of mountains, as is the case for Xibalbá, to initiate high precipitation over many parts of Mesoamerica, causing the dry conditions that lasted from 1400 to 1600 CE. The end of the MDE c. 1600 CE and the recovery to more moist conditions also ended rapidly

once the convection threshold over the oceans was reached again. Simulations with a fully reconstructed LIA climate state would be needed to fully evaluate this hypothesis.

4.4. The Role of External Forcing Factors

Volcanic eruptions and changes in solar irradiance have been discussed as major external forcing factors contributing to reinforcing ocean/sea-ice/atmosphere feedback processes in the North Atlantic during the LIA and other major dry episodes in Mesoamerica (e.g., Burn & Palmer, 2014; Steinman et al., 2022; Vieten, Warken, Zanchettin, et al., 2024; Warken et al., 2021; Winter et al., 2015). However, we find no evidence in our record of any robust response to individual volcanic eruptions nor cumulative volcanic forcing before the MDE (Figure 3e). The MDE may be a delayed response to the earlier cluster of very strong volcanic eruptions in the 13th century (Amaya et al., 2018), which would require a long-term mechanism to establish a causal relationship. The MDE also encompasses the Spörer Minimum of solar activity (1460–1550 CE, Jungclaus et al., 2017), which was associated with comparably cold temperatures in the North Atlantic (Moffa-Sánchez et al., 2014). Low solar irradiance is suggested to promote the development of frequent and persistent atmospheric blocking events over the North Atlantic, and could have contributed to the North Atlantic LIA cooling through ocean-sea ice-atmosphere feedbacks (Moffa-Sánchez et al., 2014). However, the solar connection remains elusive as prominent minima such as Wolf (1280–1350 CE), Maunder (1645–1715 CE) or Dalton (1790–1820 CE) appear only as minor dry periods in the GU-Xi-1 record (Figure 4). Hence, the phase of low solar activity may be thus implicated in the MDE, but this would require invoking strong feedbacks triggering the persistently dry conditions in Mesoamerica. Climate models can support attribution and dynamical interpretation of the reconstructed MDE. However, the multi-model ensemble used in Winter et al. (2015) revealed substantial uncertainties affecting the simulation of Yucatan precipitation, which were traced back to considerable deficiencies in the representation of key processes and in the imposed external forcing reconstructions. We leave such proxy-model comparisons to a follow-up study that should possibly also include large ensembles and single-forcing experiments.

5. Conclusions

Multiple lines of evidence from speleothem GU-Xi-1 show an extended drying event that occurred in Guatemala from 1400 to 1600 CE. Similar variations are found in some other proxy-based reconstructions, suggesting that this interval was not only restricted to the location of Xibalbá. The beginning of the MDE in our record superposes, within age error, to recent estimates of the start of the LIA, suggesting a link between the two events. The abrupt drying and cooling observed in the Xibalbá record suggests that during the MDE, Caribbean SSTs could not go over a convection threshold which explains why precipitation was strongly diminished over Mesoamerica. We find no robust connection with volcanic and solar forcing.

Our results show that the LIA in Mesoamerica was characterized by cooler SSTs and persistent drought, and highlight the important, complex role of basin-wide ocean-atmosphere interactions in regional climate variability of the historical past. Our high-resolution reconstruction reveals the possible “abrupt” character of climate transitions. We need to gain more information on past decadal regional climate variability to unveil threshold behavior and possible tipping points.

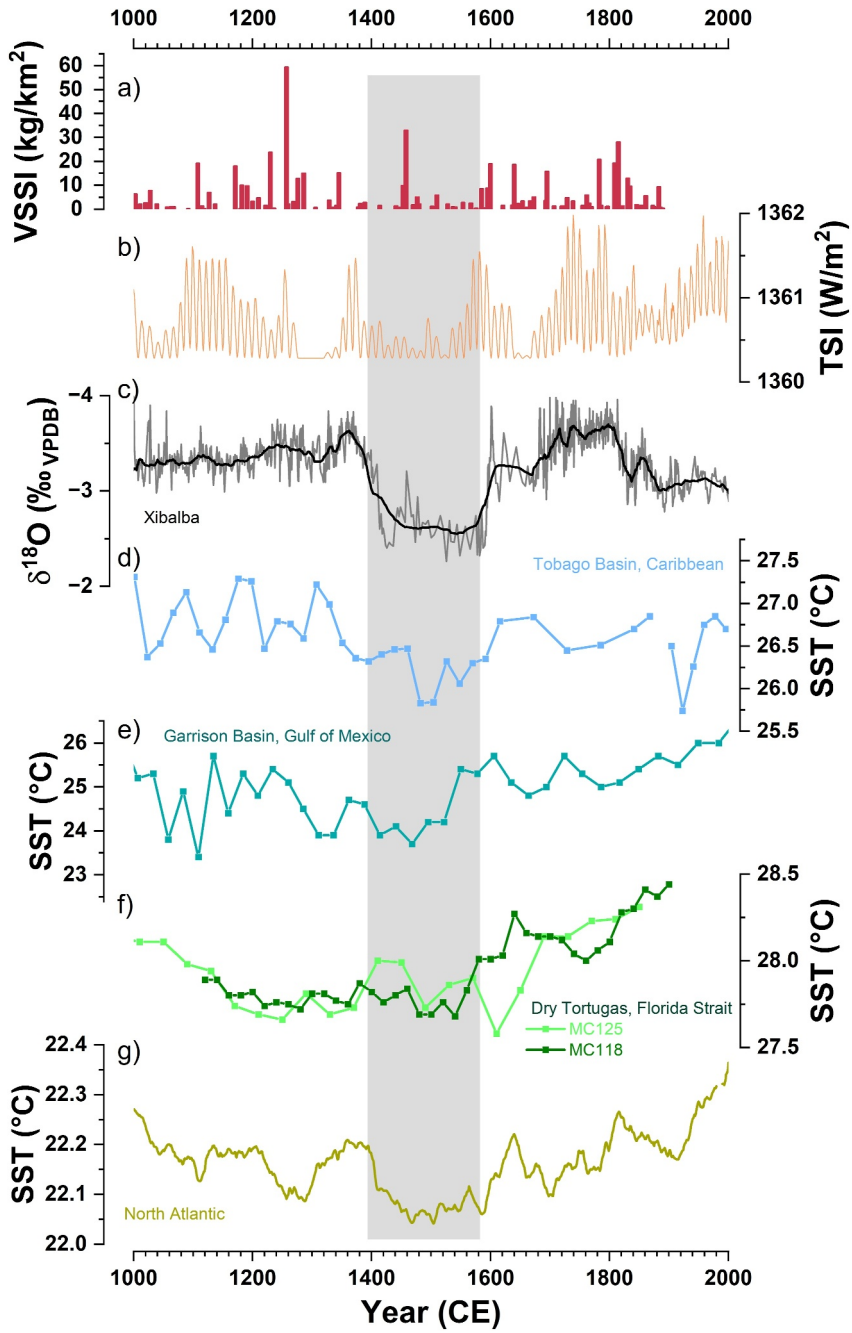

Figure 4. Comparison between the GU-Xi-1 record (c) with relevant mostly oceanic sea-surface temperature (SST) records and external forcing reconstructions. (a) evolve2k volcanic stratospheric sulfur injection rate (Jungclaus et al., 2017), (b) Total Solar Irradiance (Schmidt et al., 2011), (c) Xibalbá cave δ^{18}O record (1, this study), (d) SST Tobago Basin, Caribbean sea (6, Zhuravleva et al., 2023), (e) SST Garrison Basin, Gulf of Mexico (7, Thirumalai et al., 2018), (f) SST Dry Tortugas, Gulf of Mexico (8, Lund & Curry, 2006), (g) SST North Atlantic (9, Lapointe et al., 2020). Individual numbers before each reference refer to location of record in Figure 2 where applicable.

Data Availability Statement

The data provided as supporting material to this manuscript (GU-Xi-1_stable_isotopes.xlsx) and is deposited at the open access repository Zenodo (Winter et al., 2025).

Acknowledgments
A.W. and M.L. acknowledge support by the Visiting Scholar program of the University Ca'Foscari of Venice. Supported by NSF Grants AGS-1804263 (UNLV) and ATM-1003502 (UPRM), and facility support to UNLV via EAR-0521196. SW acknowledges support by Heidelberg University via the Olympia Morata program. We thank three anonymous reviewers for their insightful comments. We thank Sebastian Breitenbach and Gerald Haug for their help during the initial stages of this project.

References

Acuña-Soto, R., Stahle, D. W., Cleaveland, M. K., & Therrell, M. D. (2002). Megadrought and megadeath in 16th century Mexico. *Emerging Infectious Diseases*, *8*(4), 360–362. https://doi.org/10.3201/eid0804.010175

Akers, P. D., Brook, G. A., Railsback, L. B., Cherkinksy, A., Liang, F., Ebert, C. E., et al. (2019). Integrating U-Th, ^{14}C, and ^{210}Pb methods to produce a chronologically reliable isotope record for the Belize River Valley Maya from a low-uranium stalagmite. *The Holocene*, *29*(7), 1234–1248. https://doi.org/10.1177/0959683619838047

Amaya, D. J., Siler, N., Xie, S.-P., & Miller, A. J. (2018). The interplay of internal and forced modes of Hadley cell expansion: Lessons from the global warming hiatus. *Climate Dynamics*, *51*(1–2), 305–319. https://doi.org/10.1007/s00382-017-3921-5

Asmerom, Y., Baldini, J. U., Prufer, K. M., Polyak, V. J., Ridley, H. E., Aquino, V. V., et al. (2020). Intertropical convergence zone variability in the neotropics during the common era. *Science Advances*, *6*(7), eaax3644. https://doi.org/10.1126/sciadv.aax3644

Baker, A., Hartmann, A., Duan, W., Hankin, S., Comas-Bru, L., Cuthbert, M. O., et al. (2019). Global analysis reveals climatic controls on the oxygen isotope composition of cave drip water. *Nature Communications*, *10*(1), 2984. https://doi.org/10.1038/s41467-019-11027-w

Bernal, J., Revolorio, F., Cu-Xi, M., Lases-Hernández, F., Piacsek, P., Lachniet, M. S., et al. (2023). Variability of trace-elements and δ^{18}O in drip water from Gruta del Rey Marcos, Guatemala; seasonal and environmental effects, and its implications for paleoclimate reconstructions. *Frontiers in Earth Science*, *11*, 1112957. https://doi.org/10.3389/feart.2023.1112957

Bhattacharya, T., & Coats, S. (2020). Atlantic-Pacific gradients drive last millennium hydroclimate variability in Mesoamerica. *Geophysical Research Letters*, *47*(13), e2020GL088061. https://doi.org/10.1029/2020gl088061

Blaauw, M., & Christen, J. A. (2011). Flexible paleoclimate age-depth models using an autoregressive gamma process. *Bayesian Anal*, *6*(3), 457–474. https://doi.org/10.1214/11-ba618

Black, D. E., Abahazi, M. A., Thunell, R. C., Kaplan, A., Tappa, E. J., & Peterson, L. C. (2007). An 8-century tropical Atlantic SST record from the Cariaco Basin: Baseline variability, twentieth-century warming, and Atlantic hurricane frequency. *Paleoceanography*, *22*(4), PA4204. https://doi.org/10.1029/2007pa001427

Black, D. E., Peterson, L. C., Overpeck, J. T., Kaplan, A., Evans, M. N., & Kashgarian, M. (1999). Eight centuries of north atlantic ocean atmosphere variability. *Science*, *286*(5445), 1709–1713. https://doi.org/10.1126/science.286.5445.1709

Breitenbach, S. F., & Bernasconi, S. M. (2011). Carbon and oxygen isotope analysis of small carbonate samples (20 to 100 μg) with a GasBench II preparation device. *Rapid Communications in Mass Spectrometry*, *25*(13), 1910–1914. https://doi.org/10.1002/rcm.5052

Breitenbach, S. F., Rehfeld, K., Goswami, B., Baldini, J., Ridley, H., Kennett, D., et al. (2012). Constructing proxy records from age models (COPRA). *Climate of the Past*, *8*(5), 1765–1779. https://doi.org/10.5194/cp-8-1765-2012

Burn, M. J., & Palmer, S. E. (2014). Solar forcing of Caribbean drought events during the last millennium. *Journal of Quaternary Science*, *29*(8), 827–836. https://doi.org/10.1002/jqs.2660

Carlson, P. E., Noronha, A. L., Banner, J. L., Jenson, J. W., Moore, M. W., Partin, J. W., et al. (2020). Constraining speleothem oxygen isotope disequilibrium driven by rapid CO_2 degassing and calcite precipitation: Insights from monitoring and modeling. *Geochimica et Cosmochimica Acta*, *284*, 222–238. https://doi.org/10.1016/j.gca.2020.06.012

Cheng, H., Edwards, R. L., Shen, C.-C., Polyak, V. J., Asmerom, Y., Woodhead, J., et al. (2013). Improvements in ^{230}Th dating, ^{230}Th and ^{234}U half-life values, and U--Th isotopic measurements by multi-collector inductively coupled plasma mass spectrometry. *Earth and Planetary Science Letters*, *371*, 82–91.

Consortium, P. H. k. (2017). Comparing proxy and model estimates of hydroclimate variability and change over the Common Era. *Climate of the Past*, *13*(12), 1851–1900. https://doi.org/10.5194/cp-13-1851-2017

Cuna, E., Zawisza, E., Caballero, M., Ruiz-Fernández, A. C., Lozano-García, S., & Alcocer, J. (2014). Environmental impacts of Little Ice Age cooling in central Mexico recorded in the sediments of a tropical alpine lake. *Journal of Paleolimnology*, *51*, 1–14. https://doi.org/10.1007/s10933-013-9748-0

Dansgaard, W. (1964). Stable isotopes in precipitation. *Tellus*, *16*(4), 436–468. https://doi.org/10.1111/j.2153-3490.1964.tb00181.x

Deininger, M., Fohlmeister, J., Scholz, D., & Mangini, A. (2012). Isotope disequilibrium effects: The influence of evaporation and ventilation effects on the carbon and oxygen isotope composition of speleothems -- A model approach. *Geochimica et Cosmochimica Acta*, *96*, 57–79. https://doi.org/10.1016/j.gca.2012.08.013

de Menocal, P., Ortiz, J., Guilderson, T., & Sarnthein, M. (2000). Coherent high- and low-latitude climate variability during the holocene warm period. *Science*, *288*(5474), 2198–2202. https://doi.org/10.1126/science.288.5474.2198

Douglas, P. M., Pagani, M., Brenner, M., Hodell, D. A., & Curtis, J. H. (2012). Aridity and vegetation composition are important determinants of leaf-wax δD values in southeastern Mexico and Central America. *Geochimica et Cosmochimica Acta*, *97*, 24–45. https://doi.org/10.1016/j.gca.2012.09.005

Fensterer, C., Scholz, D., Hoffmann, D., Mangini, A., & Pajón, J. M. (2010). ^{230}Th/U-dating of a late Holocene low uranium speleothem from Cuba. In *IOP Conference Series: Earth and Environmental Science*. IOP Publishing, Vol. 9(1), 012015. https://doi.org/10.1088/1755-1315/9/1/012015

Fensterer, C., Scholz, D., Hoffmann, D., Spötl, C., Pajón, J. M., & Mangini, A. (2012). Cuban stalagmite suggests relationship between Caribbean precipitation and the Atlantic Multidecadal Oscillation during the past 1.3 ka. *The Holocene*, 0959683612449759.

Fernández-Donado, L., González-Rouco, J., Raible, C., Ammann, C., Barriopedro, D., García-Bustamante, E., et al. (2013). Large-scale temperature response to external forcing in simulations and reconstructions of the last millennium. *Climate of the Past*, *9*(1), 393–421. https://doi.org/10.5194/cp-9-393-2013

Giannini, A., Kushnir, Y., & Cane, M. A. (2000). Interannual variability of Caribbean rainfall, ENSO, and the Atlantic Ocean. *Journal of Climate*, *13*(2), 297–311. https://doi.org/10.1175/1520-0442(2000)013<0297:ivocre>2.0.co;2

Guo, H., Deng, W., Chen, X., Zhao, J.-x., & Wei, G. (2024). Reevaluating the Little Ice Age: Novel insights from oceanic and terrestrial records on unexpected warm winters. *Quaternary Science Reviews*, *327*, 108527. https://doi.org/10.1016/j.quascirev.2024.108527

Hansen, M., Scholz, D., Schöne, B. R., & Spötl, C. (2019). Simulating speleothem growth in the laboratory: Determination of the stable isotope fractionation (δ^{13}C and δ^{18}O) between H_2O, DIC and $CaCO_3$. *Chemical Geology*, *509*, 20–44. https://doi.org/10.1016/j.chemgeo.2018.12.012

Hodell, D. A., Brenner, M., & Curtis, J. H. (2005a). Terminal Classic drought in the northern Maya lowlands inferred from multiple sediment cores in Lake Chichancanab (Mexico). *Quaternary Science Reviews*, *24*(12–13), 1413–1427. https://doi.org/10.1016/j.quascirev.2004.10.013

Hodell, D. A., Brenner, M., Curtis, J. H., Medina-González, R., Ildefonso-Chan Can, E., Albornaz-Pat, A., & Guilderson, T. P. (2005). Climate change on the Yucatan peninsula during the little ice age. *Quaternary Research*, *63*(2), 109–121. https://doi.org/10.1016/j.yqres.2004.11.004

Jaffey, A. H., Flynn, K. F., Glendenin, L. E., Bentley, W. T., & Essling, A. M. (1971). Precision measurement of half-lives and specific activities of U^{235} and U^{238}. *Physical review C*, *4*(5), 1889.

Jungclaus, J. H., Bard, E., Baroni, M., Braconnot, P., Cao, J., Chini, L. P., et al. (2017). The PMIP4 contribution to CMIP6–Part 3: The last millennium, scientific objective, and experimental design for the PMIP4 past1000 simulations. *Geoscientific Model Development*, *10*(11), 4005–4033. https://doi.org/10.5194/gmd-10-4005-2017

Kennett, D., Breitenbach, S., Haug, G., Asmerom, Y., Polyak, V., Prufer, K., & Culleton, B. Speleothem paleoclimatic reconstruction in southern Belize. (2014).

Kennett, D. J., Breitenbach, S. F., Aquino, V. V., Asmerom, Y., Awe, J., Baldini, J. U., et al. (2012). Development and disintegration of Maya political systems in response to climate change. *Science*, *338*(6108), 788–791. https://doi.org/10.1126/science.1226299

Kerber, I. K., Kontor, F., Mielke, A., Warken, S., & Frank, N. (2025). "U–Th Analysis"–open-source software dedicated to MC-ICP-MS U-series data treatment and evaluation. *Geochronology*, *7*(1), 1–13. https://doi.org/10.5194/gchron-7-1-2025

Lachniet, M. S. (2015). Are aragonite stalagmites reliable paleoclimate proxies? Tests for oxygen isotope time-series replication and equilibrium. *Bulletin*, *127*(11–12), 1521–1533. https://doi.org/10.1130/b31161.1

Lachniet, M. S., & Patterson, W. P. (2009). Oxygen isotope values of precipitation and surface waters in northern Central America (Belize and Guatemala) are dominated by temperature and amount effects. *Earth and Planetary Science Letters*, *284*(3–4), 435–446. https://doi.org/10.1016/j.epsl.2009.05.010

Lachniet, M. S., Patterson, W. P., Burns, S., Asmerom, Y., & Polyak, V. (2007). Caribbean and Pacific moisture sources on the Isthmus of Panama revealed from stalagmite and surface water $\delta^{18}O$ gradients. *Geophysical Research Letters*, *34*(1), L01708. https://doi.org/10.1029/2006gl028469

Lapointe, F., & Bradley, R. S. (2021). Little ice age abruptly triggered by intrusion of atlantic waters into the Nordic seas. *Science Advances*, *7*(51), eabi8230. https://doi.org/10.1126/sciadv.abi8230

Lapointe, F., Bradley, R. S., Francus, P., Balascio, N. L., Abbott, M. B., Stoner, J. S., et al. (2020). Annually resolved Atlantic sea surface temperature variability over the past 2,900 y. *Proceedings of the National Academy of Sciences*, *117*(44), 27171–27178. https://doi.org/10.1073/pnas.2014166117

Lases-Hernandez, F., Medina-Elizalde, M., & Benoit Frappier, A. (2020). Drip water $\delta^{18}O$ variability in the northeastern Yucatán Peninsula, Mexico: Implications for tropical cyclone detection and rainfall reconstruction from speleothems. *Geochimica et Cosmochimica Acta*, *285*, 237–256. https://doi.org/10.1016/j.gca.2020.07.008

Lases-Hernandez, F., Medina-Elizalde, M., Burns, S., & DeCesare, M. (2019). Long-term monitoring of drip water and groundwater stable isotopic variability in the Yucatán Peninsula: Implications for recharge and speleothem rainfall reconstruction. *Geochimica et Cosmochimica Acta*, *246*, 41–59. https://doi.org/10.1016/j.gca.2018.11.028

Lechleitner, F. A., Breitenbach, S. F., Rehfeld, K., Ridley, H. E., Asmerom, Y., Prufer, K. M., et al. (2017). Tropical rainfall over the last two millennia: Evidence for a low-latitude hydrologic seesaw. *Scientific Reports*, *7*(1), 45809. https://doi.org/10.1038/srep45809

Lehner, F., Born, A., Raible, C. C., & Stocker, T. F. (2013). Amplified inception of European Little Ice Age by sea ice–ocean–atmosphere feedbacks. *Journal of Climate*, *26*(19), 7586–7602. https://doi.org/10.1175/jcli-d-12-00690.1

Lozano-García, M. d. S., Caballero, M., Ortega, B., Rodríguez, A., & Sosa, S. (2007). Tracing the effects of the little ice age in the tropical lowlands of eastern Mesoamerica. *Proceedings of the National Academy of Sciences*, *104*(41), 16200–16203. https://doi.org/10.1073/pnas.0707896104

Lucia, G., Zanchettin, D., Winter, A., Cheng, H., Rubino, A., Vásquez, O. J., et al. (2024). Atlantic Ocean thermal forcing of Central American rainfall over 140,000 years. *Nature Communications*, *15*(1), 1–10. https://doi.org/10.1038/s41467-024-54856-0

Lund, D. C., & Curry, W. (2006). Florida Current surface temperature and salinity variability during the last millennium. *Paleoceanography*, *21*(2), PA2009. https://doi.org/10.1029/2005pa001218

Mann, M. E., Bradley, R. S., & Hughes, M. K. (1999). Northern hemisphere temperatures during the past millennium: Inferences, uncertainties, and limitations. *Geophysical Research Letters*, *26*(6), 759–762. https://doi.org/10.1029/1999gl900070

Mann, M. E., Zhang, Z., Rutherford, S., Bradley, R. S., Hughes, M. K., Shindell, D., et al. (2009). Global signatures and dynamical origins of the little ice age and Medieval climate anomaly. *Science*, *326*(5957), 1256–1260. https://doi.org/10.1126/science.1177303

Marchitto, T. M., & de Menocal, P. B. (2003). Late holocene variability of upper North Atlantic deep water temperature and salinity. *Geochemistry, Geophysics, Geosystems*, *4*(12), 1100. https://doi.org/10.1029/2003GC000598

Martinez, C., Goddard, L., Kushnir, Y., & Ting, M. (2019). Seasonal climatology and dynamical mechanisms of rainfall in the Caribbean. *Climate Dynamics*, *53*(1), 825–846. https://doi.org/10.1007/s00382-019-04616-4

Matthews, J. A., & Briffa, K. R. (2005). The 'little ice age': Re-evaluation of an evolving concept. *Geografiska Annaler - Series A: Physical Geography*, *87*(1), 17–36. https://doi.org/10.1111/j.0435-3676.2005.00242.x

Medina-Elizalde, M., Burns, S. J., Lea, D. W., Asmerom, Y., von Gunten, L., Polyak, V., et al. (2010). High resolution stalagmite climate record from the Yucatán Peninsula spanning the Maya terminal classic period. *Earth and Planetary Science Letters*, *298*(1–2), 255–262. https://doi.org/10.1016/j.epsl.2010.08.016

Mendoza, B., Jáuregui, E., Diaz-Sandoval, R., García-Acosta, V., Velasco, V., & Cordero, G. (2005). Historical droughts in central Mexico and their relation with El Niño. *Journal of Applied Meteorology and Climatology*, *44*(5), 709–716.

Metcalfe, S. E., Jones, M. D., Davies, S. J., Noren, A., & MacKenzie, A. (2010). Climate variability over the last two millennia in the North American Monsoon region, recorded in laminated lake sediments from Laguna de Juanacatlán, Mexico. *The Holocene*, *20*(8), 1195–1206. https://doi.org/10.1177/0959683610371994

Mickler, P. J., Stern, L. A., & Banner, J. L. (2006). Large kinetic isotope effects in modern speleothems. *Geological Society of America Bulletin*, *118*(1–2), 65–81. https://doi.org/10.1130/B25698.1

Moffa-Sánchez, P., Born, A., Hall, I. R., Thornalley, D. J., & Barker, S. (2014). Solar forcing of North Atlantic surface temperature and salinity over the past millennium. *Nature Geoscience*, *7*(4), 275–278. https://doi.org/10.1038/ngeo2094

Moffa-Sánchez, P., & Hall, I. R. (2017). North Atlantic variability and its links to European climate over the last 3000 years. *Nature Communications*, *8*(1), 1726. https://doi.org/10.1038/s41467-017-01884-8

Moffa-Sánchez, P., Moreno-Chamarro, E., Reynolds, D., Ortega, P., Cunningham, L., Swingedouw, D., et al. (2019). Variability in the northern North Atlantic and Arctic oceans across the last two millennia: A review. *Paleoceanography and Paleoclimatology*, *34*(8), 1399–1436. https://doi.org/10.1029/2018pa003508

Noncent, D., Sifeddine, A., Emmanuel, E., Cormier, M. H., Briceño-Zuluaga, F. J., Valdés, J., et al. (2023). A 1000-year record of paleoclimate and paleoenvironment change inferred from sedimentary organic matter in Lake Azuei, Haiti. *Palaeogeography, Palaeoclimatology, Palaeoecology*, *632*, 111845. https://doi.org/10.1016/j.palaeo.2023.111845

Nyberg, J., Kuijpers, A., Malmgren, B. A., & Kunzendorf, H. (2001). Late Holocene changes in precipitation and hydrography recorded in marine sediments from the northeastern Caribbean Sea. *Quaternary Research*, *56*(1), 87–102. https://doi.org/10.1006/qres.2001.2249

Nyberg, J., Malmgren, B. A., Kuijpers, A., & Winter, A. (2002). A centennial-scale variability of tropical North Atlantic surface hydrography during the late Holocene. *Palaeogeography, Palaeoclimatology, Palaeoecology*, *183*(1–2), 25–41. https://doi.org/10.1016/s0031-0182(01)00446-1

Obrist-Farner, J., Steinman, B. A., Stansell, N. D., & Maurer, J. (2023). Incoherency in Central American hydroclimate proxy records spanning the last millennium. *Paleoceanography and Paleoclimatology*, *38*(3), e2022PA004445. https://doi.org/10.1029/2022pa004445

Oster, J. L., Warken, S. F., Sekhon, N., Arienzo, M. M., & Lachniet, M. (2019). Speleothem paleoclimatology for the caribbean, Central America, and north America. *Quaternary*, *2*(1), 5. https://doi.org/10.3390/quat2010005

Railsback, L. B., Akers, P. D., Wang, L., Holdridge, G. A., & Voarintsoa, N. R. (2013). Layer-bounding surfaces in stalagmites as keys to better paleoclimatological histories and chronologies. *International Journal of Speleology*, *42*(3), 167–180. https://doi.org/10.5038/1827-806x.42.3.1

Rauscher, S. A., Giorgi, F., Diffenbaugh, N. S., & Seth, A. (2008). Extension and intensification of the Meso-American mid-summer drought in the twenty-first century. *Climate Dynamics*, *31*(5), 551–571. https://doi.org/10.1007/s00382-007-0359-1

Richey, J. N., Poore, R. Z., Flower, B. P., Quinn, T. M., & Hollander, D. J. (2009). Regionally coherent little ice age cooling in the atlantic warm pool. *Geophysical Research Letters*, *36*(21), Artn L21703. https://doi.org/10.1029/2009gl040445

Rosenmeier, M. F., Hodell, D. A., Brenner, M., Curtis, J. H., & Guilderson, T. P. (2002). A 4000-year lacustrine record of environmental change in the southern Maya lowlands, Petén, Guatemala. *Quaternary Research*, *57*(2), 183–190. https://doi.org/10.1006/qres.2001.2305

Rosenmeier, M. F., Hodell, D. A., Brenner, M., Curtis, J. H., Martin, J. B., Anselmetti, F. S., et al. (2002). Influence of vegetation change on watershed hydrology: Implications for paleoclimatic interpretation of lacustrine δ 18 O records. *Journal of Paleolimnology*, *27*, 117–131.

Schmidt, G. A., Jungclaus, J. H., Ammann, C. M., Bard, E., Braconnot, P., Crowley, T. J., et al. (2011). Climate forcing reconstructions for use in PMIP simulations of the last millennium (v1.0). *Geoscientific Model Development*, *4*(1), 33–45. https://doi.org/10.5194/gmd-4-33-2011

Seager, R., Ting, M., Davis, M., Cane, M., Naik, N., Nakamura, J., et al. (2009). Mexican drought: An observational modeling and tree ring study of variability and climate change. *Atmósfera*, *22*(1), 1–31.

Simms, A. R., Bentley, M. J., Simkins, L. M., Zurbuchen, J., Reynolds, L. C., DeWitt, R., & Thomas, E. R. (2021). Evidence for a "little ice age" glacial advance within the Antarctic peninsula–examples from glacially-overrun raised beaches. *Quaternary Science Reviews*, *271*, 107195. https://doi.org/10.1016/j.quascirev.2021.107195

Skiba, V., & Fohlmeister, J. (2023). Contemporaneously growing speleothems and their value to decipher in-cave processes–A modelling approach. *Geochimica et Cosmochimica Acta*, *348*, 381–396. https://doi.org/10.1016/j.gca.2023.03.016

Slawinska, J., & Robock, A. (2018). Impact of volcanic eruptions on decadal to centennial fluctuations of Arctic sea ice extent during the last millennium and on initiation of the Little Ice Age. *Journal of Climate*, *31*(6), 2145–2167. https://doi.org/10.1175/jcli-d-16-0498.1

Stahle, D. W., Diaz, J. V., Burnette, D. J., Paredes, J. C., Heim Jr, R. R., Fye, F. K., et al. (2011). Major Mesoamerican droughts of the past millennium. *Geophysical Research Letters*, *38*(5), L05703. https://doi.org/10.1029/2010gl046472

Steinman, B. A., Stansell, N. D., Mann, M. E., Cooke, C. A., Abbott, M. B., Vuille, M., et al. (2022). Interhemispheric antiphasing of neotropical precipitation during the past millennium. *Proceedings of the National Academy of Sciences*, *119*(17), e2120015119. https://doi.org/10.1073/pnas.2120015119

Taylor, M. A., Whyte, F. S., Stephenson, T. S., & Campbell, J. D. (2013). Why dry? Investigating the future evolution of the Caribbean low level jet to explain projected Caribbean drying. *International Journal of Climatology*, *33*(3), 784–792. https://doi.org/10.1002/joc.3461

Thirumalai, K., Quinn, T. M., Okumura, Y., Richey, J. N., Partin, J. W., Poore, R. Z., & Moreno-Chamarro, E. (2018). Pronounced centennial-scale Atlantic Ocean climate variability correlated with Western Hemisphere hydroclimate. *Nature Communications*, *9*(1), 392. https://doi.org/10.1038/s41467-018-02846-4

Treble, P. C., Baker, A., Abram, N. J., Hellstrom, J. C., Crawford, J., Gagan, M. K., et al. (2022). Ubiquitous karst hydrological control on speleothem oxygen isotope variability in a global study. *Communications Earth and Environment*, *3*(1), 29. https://doi.org/10.1038/s43247-022-00347-3

Vieten, R., Warken, S., Winter, A., Scholz, D., Miller, T., Spötl, C., & Schröder-Ritzrau, A. (2018). Monitoring of cueva larga, Puerto Rico—A first step to decode speleothem climate records. In W. B. White, J. S. Herman, E. K. Herman, & M. Rutigliano (Eds.), *Karst groundwater contamination and public health* (pp. 319–331). Springer International Publishing. https://doi.org/10.1007/978-3-319-51070-5_36

Vieten, R., Warken, S., Winter, A., Schröder-Ritzrau, A., Scholz, D., & Spötl, C. (2018). Hurricane impact on seepage water in larga cave, Puerto Rico. *Journal of Geophysical Research-Biogeosciences*, *123*(3), 879–888. https://doi.org/10.1002/2017jg004218

Vieten, R., Warken, S. F., Winter, A., Scholz, D., Zanchettin, D., Black, D., & Lachniet, M. (2024). A sequence of abrupt climate fluctuations in the northern Caribbean related to the 8.2 ka event. *The Holocene*, *34*(3), 325–337. https://doi.org/10.1177/09596836231211874

Vieten, R., Warken, S. F., Zanchettin, D., Winter, A., Scholz, D., Black, D., et al. (2024). Northeastern Caribbean rainfall variability linked to solar and volcanic forcing. *Paleoceanography and Paleoclimatology*, *39*(4), e2023PA004720. https://doi.org/10.1029/2023pa004720

Wang, C., Zhang, L., & Lee, S.-K. (2013). Response of freshwater flux and sea surface salinity to variability of the Atlantic warm pool. *Journal of Climate*, *26*(4), 1249–1267. https://doi.org/10.1175/jcli-d-12-00284.1

Wang, C. Z., Enfield, D. B., Lee, S. K., & Landsea, C. W. (2006). Influences of the Atlantic warm pool on western hemisphere summer rainfall and Atlantic hurricanes. *Journal of Climate*, *19*(12), 3011–3028. https://doi.org/10.1175/Jcli3770.1

Warken, S., Schorndorf, N., Stinnesbeck, W., Hennhoefer, D., Stinnesbeck, S., Förstel, J., et al. (2021). Solar forcing of early holocene droughts on the Yucatán peninsula. *Scientific Reports*, *11*(13885), 13885. https://doi.org/10.1038/s41598-021-93417-z

Warken, S. F., Vieten, R., Winter, A., Spötl, C., Miller, T. E., Jochum, K. P., et al. (2020). Persistent link between caribbean precipitation and atlantic ocean circulation during the last glacial revealed by a speleothem record from Puerto Rico. *Paleoceanography and Paleoclimatology*, *35*(11), e2020PA003944. https://doi.org/10.1029/2020PA003944

Williams, I. N., Pierrehumbert, R. T., & Huber, M. (2009). Global warming, convective threshold and false thermostats. *Geophysical Research Letters*, *36*(21), L21805. https://doi.org/10.1029/2009gl039849

Winter, A., Ishioroshi, H., Watanabe, T., Oba, T., & Christy, J. (2000). Caribbean sea surface temperatures: Two-to-three degrees cooler than present during the Little Ice Age. *Geophysical Research Letters*, *27*(20), 3365–3368. https://doi.org/10.1029/2000gl011426

Winter, A., Miller, T., Kushnir, Y., Sinha, A., Timmermann, A., Jury, M. R., et al. (2011). Evidence for 800 years of North Atlantic multi-decadal variability from a Puerto Rican speleothem. *Earth and Planetary Science Letters*, *308*(1–2), 23–28. https://doi.org/10.1016/j.epsl.2011.05.028

Winter, A., Warken, S., Zanchettin, D., Lachniet, M., Rubino, A., Thomas, E. M., & Cheng, H. (2025). Supplementary data to Winter et al. (2025) "Evidence for persistent drought over Mesoamerica between 1400-1600 CE" [Dataset]. *Zenodo*. https://doi.org/10.5281/zenodo.16964592

Winter, A., Zanchettin, D., Lachniet, M., Vieten, R., Pausata, F. S. R., Ljungqvist, F. C., et al. (2020). Initiation of a stable convective hydroclimatic regime in Central America circa 9000 years BP. *Nature Communications*, *11*(1), 716. https://doi.org/10.1038/s41467-020-14490-y

Winter, A., Zanchettin, D., Miller, T., Kushnir, Y., Black, D., Lohmann, G., et al. (2015). Persistent drying in the tropics linked to natural forcing. *Nature Communications*, *6*(1), 7627. https://doi.org/10.1038/ncomms8627

Wogau, K. H., Arz, H. W., Böhnel, H. N., Nowaczyk, N. R., & Park, J. (2019). High resolution paleoclimate and paleoenvironmental reconstruction in the northern mesoamerican frontier for prehistory to historical times. *Quaternary Science Reviews*, *226*, 106001. https://doi.org/10.1016/j.quascirev.2019.106001

Wogau, K. H., Hoelzmann, P., Arz, H. W., & Böhnel, H. N. (2022). Paleoenvironmental conditions during the medieval climatic anomaly, the little ice age and social impacts in the oriental mesoamerican region. *Quaternary Science Reviews*, *289*, 107616. https://doi.org/10.1016/j.quascirev.2022.107616

Zhuravleva, A., Bauch, H. A., Mohtadi, M., Fahl, K., & Kienast, M. (2023). Caribbean salinity anomalies contributed to variable North Atlantic circulation and climate during the Common Era. *Science Advances*, *9*(44), eadg2639. https://doi.org/10.1126/sciadv.adg2639